

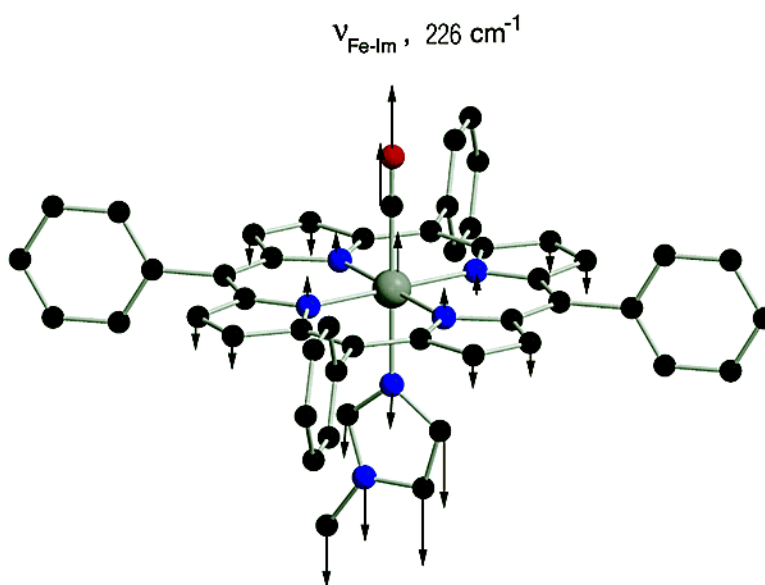
Article

Direct Determination of the Complete Set of Iron Normal Modes in a Porphyrin-Imidazole Model for Carbonmonoxy-heme Proteins: [Fe(TPP)(CO)(1-Melm)]

Brajesh K. Rai, Stephen M. Durbin, Earl W. Prohofsky, J. Timothy Sage, Mary K. Ellison, Arne Roth, W. Robert Scheidt, Wolfgang Sturhahn, and E. Ercan Alp

J. Am. Chem. Soc., **2003**, 125 (23), 6927-6936 • DOI: 10.1021/ja028219w • Publication Date (Web): 15 May 2003

Downloaded from <http://pubs.acs.org> on March 29, 2009



More About This Article

Additional resources and features associated with this article are available within the HTML version:

- Supporting Information
- Links to the 4 articles that cite this article, as of the time of this article download
- Access to high resolution figures
- Links to articles and content related to this article
- Copyright permission to reproduce figures and/or text from this article

[View the Full Text HTML](#)

Direct Determination of the Complete Set of Iron Normal Modes in a Porphyrin-Imidazole Model for Carbonmonoxy-heme Proteins: [Fe(TPP)(CO)(1-Melm)]

Brajesh K. Rai,[†] Stephen M. Durbin,^{*†} Earl W. Prohofsky,[†] J. Timothy Sage,[‡] Mary K. Ellison,[§] Arne Roth,[§] W. Robert Scheidt,[§] Wolfgang Sturhahn,^{||} and E. Ercan Alp^{||}

Contribution from the Department of Physics, Purdue University, West Lafayette, Indiana 47907, Department of Physics and Center for Interdisciplinary Research on Complex Systems, Northeastern University, Boston, Massachusetts 02115, Department of Chemistry and Biochemistry, University of Notre Dame, Notre Dame, Indiana 46556, and Advanced Photon Source, Argonne National Laboratory, Argonne, Illinois 60439

Received August 20, 2002; E-mail: durbin@physics.purdue.edu

Abstract: Detailed Fe vibrational spectra have been obtained for the heme model complex [Fe(TPP)(CO)(1-Melm)] using a new, highly selective and quantitative technique, Nuclear Resonance Vibrational Spectroscopy (NRVS). This spectroscopy measures the complete vibrational density of states for iron atoms, from which normal modes can be calculated via refinement of the force constants. These data and mode assignments can reveal previously undetected vibrations and are useful for validating predictions based on optical spectroscopies and density functional theory, for example. Vibrational modes of the iron porphyrin-imidazole compound [Fe(TPP)(CO)(1-Melm)] have been determined by refining normal mode calculations to NRVS data obtained at an X-ray synchrotron source. Iron dynamics of this compound, which serves as a useful model for the active site in the six-coordinate heme protein, carbonmonoxy-myoglobin, are discussed in relation to recently determined dynamics of a five-coordinate deoxy-myoglobin model, [Fe(TPP)(2-MeHIm)]. For the first time in a six-coordinate heme system, the iron-imidazole stretch mode has been observed, at 226 cm⁻¹. The heme in-plane modes with large contributions from the ν_{42} , ν_{49} , ν_{50} , and ν_{53} modes of the core porphyrin are identified. In general, the iron modes can be attributed to coupling with the porphyrin core, the CO ligand, the imidazole ring, and/or the phenyl rings. Other significant findings are the observation that the porphyrin ring peripheral substituents are strongly coupled to the iron doming mode and that the Fe–C–O tilting and bending modes are related by a negative interaction force constant.

I. Introduction

A wide variety of vibrational spectroscopies are applied to molecules to determine the dynamics critical to chemical reactivity and biochemical function.^{1–6} Investigations of heme proteins have especially benefitted from resonance Raman (RR) and infrared (IR) optical spectroscopies to probe the motions of the heme prosthetic group, where the focus is on the central iron atom.^{1,3,4,7} Ideally, these data are used to infer the character

of the individual normal modes of the heme molecule, and the coupling of the heme to the entire protein. Further, these assignments can be tested against theoretical models, such as those based on density functional theory (DFT).^{3,4} This entire process is limited, however, by the relatively few spectral lines whose character can be determined experimentally. Significant progress has been made by observing spectral changes due to isotope substitutions for both the iron atom and various ligands and porphyrin substituents, but even in the best cases perhaps only a few modes can be attributed to the centrally important iron atom. The new, X-ray synchrotron-based Nuclear Resonance Vibrational Spectroscopy (NRVS) can now remove this limitation by measuring the complete set of iron vibrational modes, utilizing the X-ray absorption characteristics of ⁵⁷Fe, the well-studied Mössbauer isotope.^{8–11} We present here an

[†] Department of Physics, Purdue University.

[‡] Department of Physics and Center for Interdisciplinary Research on Complex Systems, Northeastern University.

[§] Department of Chemistry and Biochemistry, University of Notre Dame.

^{||} Advanced Photon Source, Argonne National Laboratory.

- (1) Vogel, K. M.; Kozłowski, P. M.; Zgierski, M. Z.; Spiro, T. G. *J. Am. Chem. Soc.* **1999**, *121*, 9915–9921.
- (2) Goodno, G. D.; Astinov, V.; Miller, R. J. D. *J. Phys. Chem. A* **1999**, *103*, 10 630–10 643.
- (3) Rush, T. S.; Kozłowski, P. M.; Piffat, C. A.; Kumble, R.; Zgierski, M. Z.; Spiro, T. G. *J. Phys. Chem. B* **2000**, *104*, 5020–5034.
- (4) Klug, D. D.; Zgierski, M. Z.; Tse, J. S.; Liu, Z.; Kincaid, J. R.; Czarniecki, K.; Hemley, R. J. *Natl. Acad. Sci.* **2002**, *99*, 12 526–12 530.
- (5) Rosca, F.; Kumar, A. T. N.; Ye, X.; Sjodin, T.; Demidov, A. A.; Champion, P. M. *J. Phys. Chem. A* **2000**, *104*, 4280–4290.
- (6) Sage, J. T.; Durbin, S. M.; Sturhahn, W.; Wharton, D. C.; Champion, P. M.; Hession, P.; Sutter, J.; Alp, E. E. *Phys. Rev. Lett.* **2001**, *86*, 4966–4969.

- (7) Spiro, T. G. *Resonance Raman Spectra of Heme and Metalloproteins*, Volume 3 of *Biological Applications of Raman Spectroscopy*; Wiley-Interscience: New York 1988.
- (8) Seto, M.; Yoda, Y.; Kikuta, S.; Zhang, X. W.; Ando, M. *Phys. Rev. Lett.* **1995**, *74*, 3828.
- (9) Sturhahn, W.; Toellner, T. S.; Alp, E. E.; Zhang, X.; Ando, M.; Yoda, Y.; Kikuta, S.; Seto, M.; Kimball, C. W.; Dabrowski, B. *Phys. Rev. Lett.* **1995**, *74*, 3832.

application of NRVS to a heme model compound that demonstrates the ability to measure the full spectrum of iron modes and to gain a much more complete picture of heme dynamics.

The binding of carbon monoxide to myoglobin or hemoglobin is accompanied by several well-established structural changes of the heme molecule and its surroundings.^{12,13} As a result of the CO binding, the heme iron moves approximately 0.3 Å from its out-of-plane position to essentially an in-plane position. In addition, the length of the Fe–N_{e2} bond slightly decreases (N_{e2} refers to the nitrogen atom from the His imidazole, bound to the porphyrin Fe).¹⁴ Similar structural changes are also observed in heme model compounds upon binding CO.^{15,16} The transition from an out-of-plane to a planar structure is believed to be responsible for triggering the allosteric mechanism for cooperative O₂ binding in Hb.^{17–19}

To correlate structural changes with the functional properties of heme proteins, an understanding of their effect on the dynamics of the active site is necessary. Spectroscopic evidence for structural changes of the porphyrin upon binding a CO ligand to the deoxy heme is obtained from Raman “marker” lines in the high-frequency region of 1200–1600 cm⁻¹.²⁰ The marker lines, which are due to the localized vibrations of the porphyrin core, have been very well correlated with the oxidation, spin and ligand states of the heme.⁷ At lower frequency, the iron-histidine stretch ($\nu_{\text{Fe-His}}$) mode near 220 cm⁻¹ can be monitored to study the effect of ligand dissociation. Note that the Fe–N_{e2} mode, which is strongly Raman active in the deoxy state, is not observed in carbonmonoxy myoglobin or carbonmonoxy heme model compounds. The $\nu_{\text{Fe-His}}$ mode is observed only after the ligand dissociation, e.g., as a result of photolysis. The dependence of low-frequency iron vibrational modes on the heme structure is not well understood, as most iron modes are Raman inactive both in deoxy and carbonmonoxy states of myoglobin and heme models.

Using traditional optical techniques, direct observation of iron vibrations in carbonmonoxy myoglobin (MbCO) and carbonmonoxy heme model compounds is limited to the Raman active CO ligand modes, i.e., the Fe–C stretch and Fe–C–O bending modes;^{21,22} these are also accessible via FTIR studies.²³ Other important dynamics are available from IR studies; recent work has stimulated considerable discussion about the amount of CO bending away from the heme normal that can be deduced from

both IR spectroscopy and from crystallography.^{24,25,14} On the other hand, NRVS is well suited to study the biologically active iron modes that are not observed by other spectroscopic techniques.^{8–10} As there are no optical selection rules, all modes having sufficient displacement of iron are detected by this technique. Recently, Rai et al. used NRVS and normal-mode analysis to characterize iron vibrational modes of heme model compounds (nitrosyl)iron(II) tetraphenylporphyrin, [Fe(TPP)(NO)],²⁶ and (2-methylimidazole)(tetraphenylporphyrinato)iron(II), [Fe(TPP)(2-MeHIm)].²⁷ Iron normal modes of [Fe(TPP)(2-MeHIm)] are particularly interesting, as this compound mimics the active site of deoxymyoglobin. The heme model compound [Fe(TPP)(CO)(1-MeIm)], which is the subject of this paper, represents the active site of carbonmonoxy myoglobin (MbCO). A comparison of the NRVS-determined iron dynamics of the six-coordinated heme model, [Fe(TPP)(CO)(1-MeIm)], to that of the five-coordinated heme, [Fe(TPP)(2-MeHIm)], is expected to provide a better understanding of the effect of ligand binding on the functionally active modes in heme proteins.

Important findings include that the binding of CO to form [Fe(TPP)(CO)(1-MeIm)] leads to the observation of several iron modes that are weak or absent in [Fe(TPP)(2-MeHIm)]. Peripheral substituents have a large effect on the dynamics of the iron, especially for out-of-plane motions. NRVS has allowed the first identification of the Fe–His vibrational mode in a six-coordinate derivative, emphasizing the unique capabilities of the method for the study of iron-based vibrational modes.

II. Methods

This study comprised first the synthesis of ⁵⁷Fe-enriched Fe(TPP)(1-MeIm)(CO) in polycrystalline form, then NRVS data acquisition at the synchrotron, and finally a normal mode calculation where the force constants in a single molecule model were adjusted to fit the data. These procedures are described below.

A. Sample Preparation. The free base H₂TPP was prepared according to Adler et al.²⁸ ⁵⁷Fe-enriched [⁵⁷Fe(TPP)Cl] was prepared using the metalation method described by Landergren and Baltzer.²⁹ ⁵⁷Fe-enriched [⁵⁷Fe(TPP)]₂O was prepared by washing a solution of [⁵⁷Fe(TPP)Cl] in methylene chloride with 2M aqueous sodium hydroxide solution, drying the collected organic layers with sodium sulfate followed by recrystallization from methylene chloride/hexanes.

The following reaction steps were carried out under strictly anaerobic conditions. All solvents were distilled over sodium and freeze/pump/thaw degassed (at least three cycles) prior to use. Ethane thiol (Acros Organics), 1-methylimidazole (Aldrich Chemical Co.) and carbon monoxide gas (Matheson Gas Products) were used without prior purification. [⁵⁷Fe(TPP)] was obtained by stirring a solution of 90 mg (0.074 mmol) [⁵⁷Fe(TPP)]₂O and 6 mL ethane thiol in 40 mL toluene for 2 d (color change from brown-green to dark red). After the reduction a solution of 21 μL (0.27 mmol) 1-methylimidazole in 5 mL toluene was added by cannula. After stirring for 1 h, the reaction flask was purged with carbon monoxide gas and the mixture stirred overnight under carbon monoxide atmosphere. [⁵⁷Fe(TPP)(1-MeIm)CO] was precipitated by adding a 4-fold excess of hexanes. The solvents were decanted and the remaining purple solid was purged with argon for 10 min.

- (10) Sturhahn, W.; Kohn, V. G. *Hyperfine Interact.* **1999**, *123*, 367–399.
- (11) Mao, H. K.; Xu, J.; Struzhkin, V. V.; Shu, J.; Hemley, R. J.; Sturhahn, W.; Hu, M. Y.; Alp, E. E.; Vocadlo, L.; Alfe, D.; Price, G. D.; Gillan, M. J.; Schwoerer-Bohning, M.; Hansermann, D.; Eng, P.; Shen, G.; Giefers, H.; Lubbers, R.; Wortmann, G. *Science* **2001**, *292*, 914–916.
- (12) Stryer, L. *Biochemistry*, third edition; W. H. Freeman: New York, 1988.
- (13) Fermi, G. *Molecular Structures in Biology*; Oxford University Press: New York, 1993.
- (14) Kachalova, G. S.; Popov, A. N.; Bartunik, H. D. *Science* **1999**, *284*, 473–476.
- (15) Salzmann, R.; Ziegler, C. J.; Godbout, N.; McMahon, M. T.; Suslick, K. S.; Oldfield, E. *J. Am. Chem. Soc.* **1998**, *120*, 11 323–11 334.
- (16) Ellison, M. K.; Schulz, C. E.; Scheidt, W. R. *Inorg. Chem.* **2002**, *41*, 2173–2181.
- (17) Perutz, M. *Nature* **1970**, *228*, 726–739.
- (18) Scheidt, W. R.; Hoard, J. L. *J. Am. Chem. Soc.* **1973**, *95*, 8281–8288.
- (19) Hoard, J. L.; Scheidt, W. R. *Proc. Natl. Acad. Sci. U.S.A.* **1973**, *70*, 3919–3922.
- (20) Kincaid, J. R. *Resonance Raman Spectra of Heme Proteins and Model Compounds*, volume 7, of *Porphyrin Handbook*; Academic Press: New York, 2000.
- (21) Yu, N. T.; Kerr, E. A. *Biological Application of Raman Spectroscopy*; Wiley-Interscience: New York, Vol. 3, 1988.
- (22) Unno, M.; Christian, J. F.; Olson, J. S.; Sage, J. T.; Champion, P. M. *J. Am. Chem. Soc.* **1998**, *120*, 2670–2671.
- (23) Hu, S.; Vogel, K. M.; Spiro, T. G. *J. Am. Chem. Soc.* **1994**, *116*, 11 187–11 188.

- (24) Sage, J. T.; Jee, W. *J. Mol. Biol.* **1997**, *274*, 21–27.
- (25) Spiro, T. G.; Kozlowski, P. M. *J. Am. Chem. Soc.* **1998**, *120*, 4524–4525.
- (26) Rai, B. K.; Durbin, S. M.; Prohofsky, E. W.; Sage, J. T.; Wyllie, G. R. A.; Scheidt, W. R.; Sturhahn, W.; Alp, E. E. *Biophys. J.* **2002**, *82*, 2951.
- (27) Rai, B. K.; Durbin, S. M.; Prohofsky, E. W.; Sage, J. T.; Ellison, M. K.; Scheidt, W. R.; Sturhahn, W.; Alp, E. E. *Phys. Rev. E* **2002**, *66*, 51 904.
- (28) Adler, A. D.; Longo, F. R.; Finarelli, J. D.; Goldmacher, J.; Assour, J.; Korsakoff, L. *J. Org. Chem.* **1967**, *32*, 476.
- (29) Landergren, M.; Baltzer, L. *Inorg. Chem.* **1990**, *29*, 556–557.

^{57}Fe -enriched $[\text{}^{57}\text{Fe}(\text{TPP})(1\text{-MeIm})(\text{CO})]$ was characterized by IR and UV-vis spectroscopy. The Soret band varies from 422 nm in methylene chloride to 424 nm in toluene, the main visible band from 544 nm in methylene chloride to 543 nm in toluene. The CO stretch band in the IR spectrum was found to be at 1969 cm^{-1} . There were no differences in the IR spectra between KBr pellets prepared under an inert atmosphere in a drybox and samples prepared under aerobic conditions. IR spectra were unaffected by exposure to air for several days.

B. Nuclear Resonance Vibrational Spectroscopy. NRVS is a new technique that employs the unique capabilities of advanced X-ray synchrotron sources. It utilizes the Mössbauer transition in certain nuclear isotopes to observe shifts in the nuclear absorption probability caused by vibrational motions of the nuclei, from which the partial vibrational density of states can be determined. The current study is restricted to the ^{57}Fe isotope.

An X-ray can be resonantly absorbed by the nucleus when the X-ray energy E_x is within the exceedingly narrow Mössbauer line width (about 10^{-8} eV) of the resonance ($E_0 \approx 14.413\text{ keV}$). If the difference between E_x and E_0 matches the energy of a vibrational quantum of the system E_{vib} , however, then absorption can occur; e.g., if $E_x + E_{\text{vib}} = E_0$. Classically, this is analogous to a Doppler shift, where the moving nucleus sees a Doppler-shifted X-ray energy changed from E_x to E_0 .

There are two critical properties of the X-ray beam that require a specialized beamline at a third-generation X-ray synchrotron: there must be a sufficiently large number of X-ray photons within the 10^{-8} eV bandwidth to excite acceptable count rates, and this excitation beam must have an energy band-pass about E_x which is narrower than typical vibrational energies; about 1 meV (or 8 cm^{-1}) is desirable.³⁰ For the studies reported here, samples contained about 10^{18} resonant Fe atoms, and data collection required 2–4 h. (The natural ^{57}Fe concentration of 2.4% was enriched to over 90% in these samples, an essential step for reasonable data collection times.)

Iron dynamics are probed by measuring the X-ray absorption spectrum over a typical energy range of 0–700 cm^{-1} about the resonance (see Figure 1). By scanning the X-ray energy both below and above the resonance energy E_0 , the Stokes and anti-Stokes components of the absorption spectrum are obtained. This provides a direct measure of the sample temperature, and allows for the extraction of the Fe partial vibrational density of states using the PHOENIX computer program.^{10,31,26} Using the sum rules due to Lipkin,³² the measured spectrum can be normalized to determine the absolute absorption cross section as a function of energy. By assuming harmonic interactions between the Fe atom and its neighbors, the contribution from single vibrational modes can be separated from that of multiple excitations, and the Fe partial vibrational density of states (VDOS) determined. Further details of the NRVS technique and data analysis are described elsewhere.^{8,9,33–35}

Measurements were conducted at the SRI-CAT sector 3-ID-D station of the Advanced Photon Source, Argonne National Laboratory. The polycrystalline powder sample of $[\text{Fe}(\text{TPP})(\text{CO})(1\text{-MeIm})]$ was prepared by mixing with a small amount of vacuum grease and placing in a sealed cell which was directly mounted onto a He flow cryostat, and cooled to 20 K. The resonant absorption of the incident X-rays was monitored by Fe K fluorescence observed with a time-resolving Si avalanche photodiode detector.

C. Computational Details. Normal mode calculations were performed in a mass-weighted Cartesian (MWC) coordinate system.

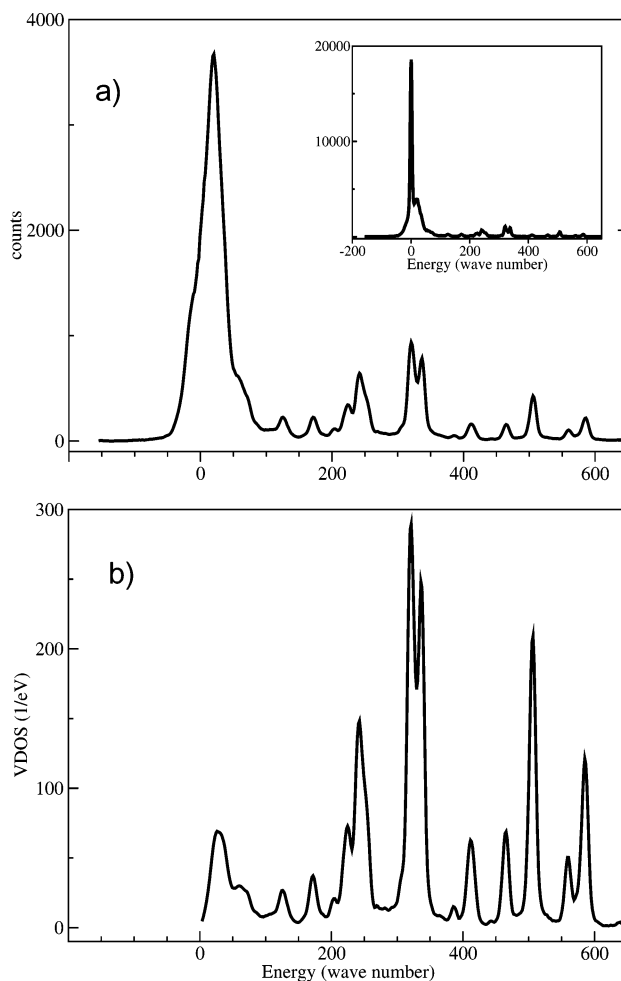


Figure 1. Nuclear resonance vibrational spectroscopy data for $[\text{Fe}(\text{TPP})(\text{CO})(1\text{-MeIm})]$ at 20 K. (a) Inset shows the complete measured NRVS data as counts versus the energy shift from resonance, measured in wavenumbers (cm^{-1}), with a large peak at the origin and weak structure on the high energy side. Main figure shows the same data after removing the central peak, using the experimentally determined resolution function. Little structure appears on the low energy side due to the lack of thermally excited vibrational modes at low temperature. (b) The experimental Fe partial vibrational density of states (VDOS) extracted from these data.

Structural parameters for the $[\text{Fe}(\text{TPP})(\text{CO})(1\text{-MeIm})]$ model were taken from the X-ray data of Salzmann et al.¹⁵ The structure, as shown in Figure 2, was slightly modified to maintain identical structure for each of the four pyrroles and phenyls. In addition, the porphyrin core of the model structure was set to be coplanar, with the iron at the center. The phenyls were oriented perpendicular to the porphyrin plane. The fifth iron ligand, the imidazole ring, is placed in such a way that the $\text{Fe}-\text{N}_{\text{im}}$ bond is along the heme normal. The projection of the imidazole plane (azimuthal angle) on the porphyrin makes an angle of 20° from the closest $\text{Fe}-\text{N}_p$ bond. The $\text{Fe}-\text{C}$ bond of the CO ligand was oriented perpendicular to the heme plane. In agreement with the X-ray data, the $\text{Fe}-\text{C}-\text{O}$ angle was set to 179° with the projection of $\text{Fe}-\text{C}-\text{O}$ plane on the porphyrin making an angle of 19° from the closest $\text{Fe}-\text{N}_p$ bond.

The initial set of force constants was transferred from previous work on similar heme model compounds.^{3,27} These included the Wilson type force fields such as bond stretch, angle bend, torsion, and out-of-plane bend.³⁶ Other terms involving interactions between stretch–stretch, stretch–bend, and bend–bend force constants were also used in describing the potential energy of the $[\text{Fe}(\text{TPP})(\text{CO})(1\text{-MeIm})]$ system.

(30) Toellner, T. S.; Hu, M. Y.; Sturhahn, W.; Quast, K.; Alp, E. E. *Appl. Phys. Lett.* **1997**, *71*, 2112–2114.

(31) Sturhahn, W. *Hyperfine Interact.* **2000**, *125*, 149–172.

(32) Lipkin, H. J. *Phys. Rev. B* **1995**, *52*, 10073.

(33) Keppler, C.; Achterhold, K.; Ostermann, A.; vanBurck, U.; Potzel, W.; Chumakov, A.; Baron, A. Q. R.; Ruffer, R.; Parak, F. *Eur. Biophys. J.* **1997**, *25*, 221–224.

(34) Chumakov, A. I.; Sturhahn, W. *Hyperfine Int.* **1999**, *123*, 781–808.

(35) Sage, J. T.; Paxson, C.; Wyllie, G. R. A.; Sturhahn, W.; Durbin, S. M.; Champion, P. M.; Alp, E. E.; Scheidt, W. R. *J. Phys.: Condens. Matter* **2001**, *13*, 7707–7722.

(36) Wilson, E. B.; Decius, J. C.; Cross, P. C. *Molecular Vibrations*; McGraw-Hill Book Co.: New York, 1955.

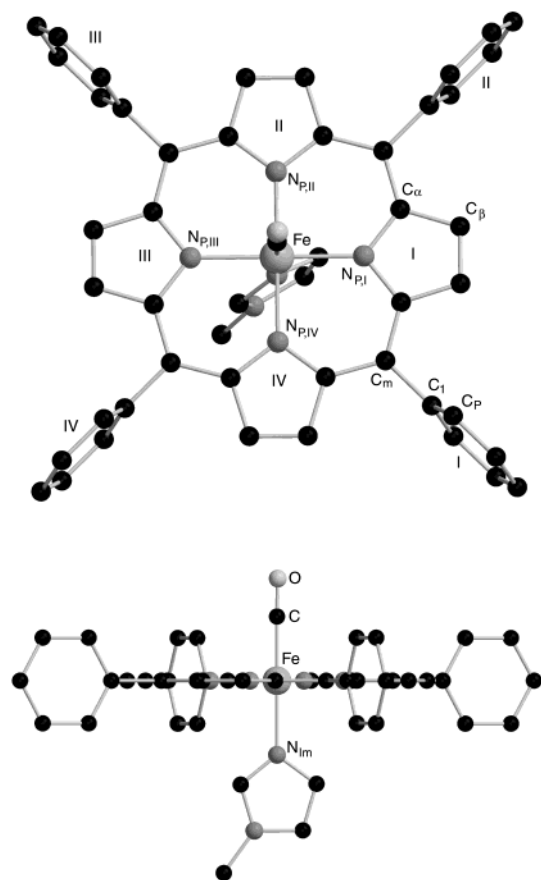


Figure 2. Structure of the model [Fe(TPP)(CO)(1-MeIm)], top (Top) and side (Bottom) views. For clarity, the beta hydrogens and the hydrogen atoms on the phenyl rings have been omitted.

The normal mode calculation using the initial force constants gave an iron vibrational density of states (VDOS) which was in rough agreement with the observed spectrum. The force fields were refined to obtain a better fit between the experimental and calculated iron VDOS of [Fe(TPP)(CO)(1-MeIm)]. An iterative method based on the Jacobian-Determinant method was used for refinement.³⁷ In addition, several force constants were also adjusted manually to get a better fit of the calculation with the experimental data.

To make a meaningful comparison of our normal mode calculation with the NRVS data, it is necessary to convert the normal mode spectrum into the iron VDOS, following the method described by Rai et al.²⁶ The iron VDOS depends on the inelastic nuclear absorption probability, which in turn is a function of Fe displacements and vibrational energy associated with the normal modes of the system.^{9,38}

The [Fe(TPP)(CO)(1-MeIm)] normal modes are classified by calculating their overlaps with a set of selected reference vectors and from their potential energy distributions (PED). The PED of a normal mode gives information on the contribution of each force constant to its potential energy. A detailed discussion of the classification schemes for the vibrational modes is given in Section IV.

III. Experimental Results

The NRVS measurements on the polycrystalline powder sample of [Fe(TPP)(CO)(1-MeIm)] were performed at 20 K. The measured spectrum was subsequently converted to give iron VDOS using the PHOENIX computer program.¹⁰ Figure 3 shows the iron VDOS of [Fe(TPP)(CO)(1-MeIm)] in an energy range of 0–700 cm^{-1} . The widths

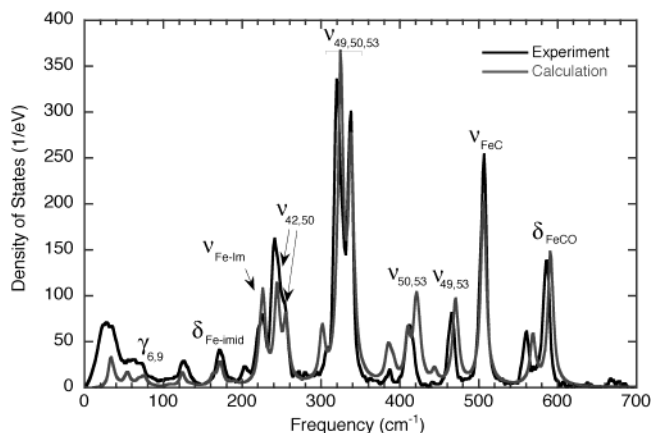


Figure 3. Measured and calculated iron VDOS of polycrystalline powder sample of [Fe(TPP)(CO)(1-MeIm)]. The calculated VDOS is multiplied by an arbitrary scale factor.

of the observed peaks are limited by the experimental resolution of 7 cm^{-1} (0.85 meV), except at very low energy. A peak in the VDOS is proportional to the squared maximum displacement of the Fe atom at that frequency, weighted linearly by the energy. Thus, for two vibrational features of identical size and shape in the VDOS, the one at the lower energy will involve a larger iron amplitude. The VDOS derived from the [Fe(TPP)(CO)(1-MeIm)] data represents an average over the randomly oriented heme molecules of the polycrystalline sample.

The spectrum contains a number of well resolved lines that show little evidence of dispersion. A comparison of the iron vibrational spectrum of 6-coordinate [Fe(TPP)(CO)(1-MeIm)] with that of 5-coordinate compound [Fe(TPP)(2-MeHIm)], as shown in Figure 4, indicates the activation of several iron modes due to CO binding to the porphyrin iron. The observed iron modes of [Fe(TPP)(CO)(1-MeIm)] are in general sharper and more numerous than those seen for [Fe(TPP)(2-MeHIm)]. More and sharper lines are also seen in 5-coordinate [Fe(TPP)(NO)] (see Figure 4), so this seems to be correlated with the presence of a diatomic ligand.

Most of the vibrational modes seen here are not observed in Raman measurements because they are Raman inactive, as discussed below. However, Raman lines corresponding to the Fe–C stretch and Fe–C–O bending modes have been widely observed near 500 and 580 cm^{-1} ,^{22,39,40} respectively, in agreement with the NRVS spectrum. Although a confident assignment of the observed iron vibrational modes requires a normal mode calculation, some important insight about these modes can still be obtained by a comparison of [Fe(TPP)(CO)(1-MeIm)] iron modes to those of [Fe(TPP)(2-MeHIm)] and [Fe(TPP)(NO)]. A direct correlation between several [Fe(TPP)(CO)(1-MeIm)] modes to those of [Fe(TPP)(2-MeHIm)] and [Fe(TPP)(NO)] can be made, as shown in Figure 4. The strongest feature in the VDOS of [Fe(TPP)(CO)(1-MeIm)], the pair of modes at 319 and 341 cm^{-1} , is strikingly similar to that observed for [Fe(TPP)(NO)], both in terms of their energies and relative amplitudes; these pair of modes have been found to show substantial overlap with in-plane ν_{53} and ν_{50} vibrations of the core porphyrin. A band (with at least three overlapping modes) is observed in 200–260 cm^{-1} region of [Fe(TPP)(CO)(1-MeIm)] spectrum. The experimental Fe VDOS of [Fe(TPP)(2-MeHIm)] and [Fe(TPP)(NO)] also show a number of vibrational modes in this region, which are attributed to a combination of porphyrin in-plane (primarily ν_{42} and ν_{50}) and out-of-plane modes, as well as the $\nu_{\text{Fe-im}}$ vibration (in the case of [Fe(TPP)(2-MeHIm)]).^{26,27} In the low-frequency region (0–

(37) Levin, I. W. *Vibrational Spectra and Structure*; Elsevier Scientific: New York, 1975; Vol. 4.

(38) Paulsen, H.; Winkler, H.; Trautwein, A.; Gruenstedel, H.; Rusanov, V.; Toftlund, H. *Phys. Rev. B* **1999**, *59*, 975–984.

(39) Ray, G. B.; Li, X. Y.; Ibers, J. A.; Sessler, J. L.; Spiro, T. G. *J. Am. Chem. Soc.* **1994**, *116*, 162–176.

(40) Vogel, K. M.; Kozłowski, P. M.; Zgierski, M. Z.; Spiro, T. G. *Inorg. Chim. Acta* **2000**, *297*, 11–17.

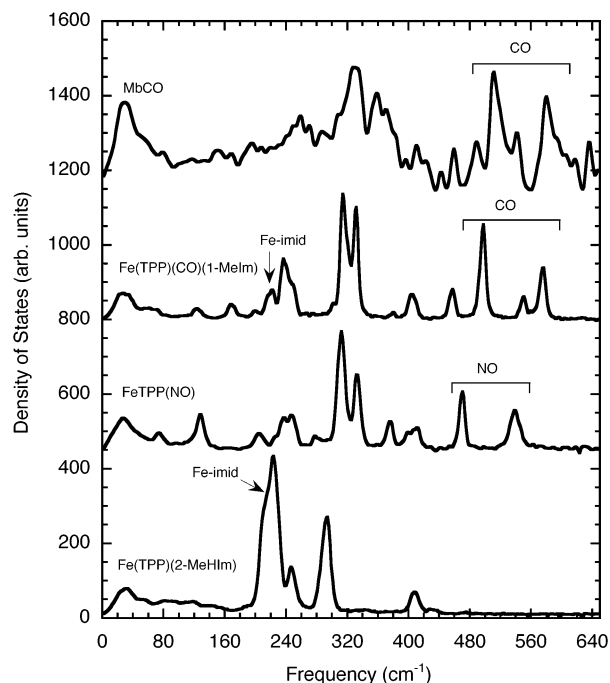


Figure 4. Comparison of Fe vibrational densities of state for 5- and 6-coordinate model compounds and the heme protein, carbonmonoxy-myoglobin (MbCO). The bottom trace is 5-coordinate [Fe(TPP)(2-MeHIm)],²⁷ showing the Fe–Imid stretch frequency near 220 cm^{-1} . Note that this spectrum has relatively few distinct peaks. Next is [Fe(TPP)(NO)],²⁶ which is also 5-coordinate, but with a diatomic ligand (NO) instead of the larger imidazole molecule. The NO bend and stretch modes are indicated by the bracket. The third trace is for [Fe(TPP)(CO)(1-MeIm)], which is 6-coordinate by both a diatomic ligand (CO) and an imidazole molecule. Clearly this spectrum is very similar to [Fe(TPP)(NO)], indicating that the presence of diatomic ligand (CO or NO) is more important than the imidazole molecule or whether the coordination is 5- or 6-fold. The top spectrum is for the MbCO protein;⁶ this has poorer signal-to-noise ratio because of the lower Fe concentration in this sample as compared with the heme model compounds. The CO bend and stretch peaks, indicated by a bracket, are similar to the other spectra. Note that all four spectra show a peak near 300 cm^{-1} , corresponding to a mode with in-plane character, e.g., ν_{53} .

50 cm^{-1}), the measured iron VDOS spectra of all three heme model compounds are essentially identical.

IV. Computational Results and Discussions

The NRVS data are converted to Fe partial vibrational density of states, effectively the complete normal mode spectrum in terms of the Fe displacements versus frequency. We desire an analysis of these normal modes that describes with reasonable confidence the character of these modes in terms of relative atomic displacements. This problem is fundamentally underdetermined because there are 85 atoms in this molecule (Figure 2), each at a specific location having effective interactions with multiple neighbors. The resulting $3(85) - 6 = 249$ nonzero normal modes of this molecule contribute to a much smaller number of measured spectral lines (Figure 1). Confidence that a given description is accurate generally follows from analyzing related model compounds and requiring consistent results.

The traditional method for metalloporphyrins, which we adopt here, has been to develop an empirical force field consisting of force constants that are adjusted to make a normal coordinate analysis (NCA) produce a good fit to available vibrational data. This has been done for a range of metalloporphyrins^{3,41–43} using data from resonance Raman scattering or infrared absorption

spectroscopy (neither of which are particularly sensitive to Fe motion in heme, unlike NRVS). More recently, however, ab initio methods have successfully been applied to molecules of the size and complexity of metalloporphyrins, in particular using the density functional theory–scaled quantum mechanical (DFT-SQM) approach.^{3,44–48} DFT methods require first that the equilibrium molecular structure be determined by energy minimization, then the corresponding set of electronic states, and finally the resultant vibrational spectra, all of which is computationally demanding for molecules approaching 85 atoms in size. A recent comparison³ of a normal coordinate analysis with DFT-SQM for [NiTPP] (with 77 atoms) found the two methods to be in “excellent agreement” for most bond stretching and angle bending force constants, with somewhat less success for off-diagonal force constants. Our normal-mode analyses of NRVS data demonstrate the necessity of including the complete molecular periphery in any DFT analysis of heme dynamics. Given the relative simplicity of a normal coordinate analysis, the near equivalence of the two methods under appropriate conditions, and the availability of NCA analyses of NRVS data from similar model compounds,^{26,27} we discuss here the results of a normal coordinate analysis on [Fe(TPP)(CO)(1-MeIm)]. Comparisons are made to DFT results on similar structures.^{1,3,39,49,50}

The 249 modes of [Fe(TPP)(CO)(1-MeIm)] with nonzero frequencies can be described according to their origin from porphyrin, phenyl, imidazole, or CO units of the system. Although the localized modes of the phenyl and imidazole units are not expected to cause any significant displacement of Fe and thus would not be detected by NRVS, modes that involve a coupling of phenyl, imidazole, or CO units with the porphyrin are observed in the iron VDOS. In addition, the in-plane and out-of-plane modes of the porphyrin core having symmetry type E_u (in-plane) and A_{2u} (out-of-plane) are also observed; these are the only symmetry types with Fe displacements.

The [Fe(TPP)(CO)(1-MeIm)] modes are classified by calculating their overlaps with a set of selected reference vectors. The elements of this set are the internal modes of the porphyrin core.^{51,52} Also included in the reference set are the coupled modes of the porphyrin-imidazole and porphyrin-CO systems. The normal coordinates describing such coupled modes are Fe–Imidazole and Fe–C stretch, and Fe– $N_{\text{Im}}-C_{\text{Im}}$ and Fe–C–O angle bend coordinates. The overlap of [Fe(TPP)(CO)(1-MeIm)] normal modes with the modes of the reference set is calculated

- (41) Li, X. Y.; Czernuszewicz, R. S.; Kincaid, J. R.; Su, Y. O.; Spiro, T. G. *J. Phys. Chem.* **1990**, *94*, 31–47.
- (42) Li, X. Y.; Czernuszewicz, R. S.; Kincaid, J. R.; Stein, P.; Spiro, T. G. *J. Phys. Chem.* **1990**, *94*, 47–61.
- (43) Hu, S.; Mukherjee, A.; Piffat, C.; Mak, R. S.; Li, X. Y.; Spiro, T. G. *Biospectroscopy* **1995**, *1*, 395–412.
- (44) Pulay, P.; Fogarosi, G.; Zhou, X.; Taylor, P. W. *Vib. Spectrosc.* **1990**, *1*, 159.
- (45) Kozłowski, P.; Z.; Zgierski, M.; Pulay, P. *Chem. Phys. Lett.* **1995**, *247*, 379–385.
- (46) Kozłowski, P. M.; Jarzecki, A. A.; Pulay, P. *J. Phys. Chem.* **1996**, *100*, 13 985–13 992.
- (47) Rush, T.; Kumble, R.; Mukherjee, A.; Blackwood, M. E.; Spiro, T. G. *J. Phys. Chem.* **1996**, *100*, 12 076–12 085.
- (48) Kumble, R.; Rush, T. S.; Blackwood, M. E.; Kozłowski, P. M.; Spiro, T. G. *J. Phys. Chem. B* **1998**, *102*, 7280–7286.
- (49) Kozłowski, P. M.; Spiro, T. G.; Zgierski, M. Z. *J. Phys. Chem. B* **2000**, *10* 659–10 666.
- (50) Kozłowski, P. M.; Vogel, K. M.; Zgierski, M. Z.; Spiro, T. G. *J. Porphyrins Phthalocyanines* **2001**, *5*, 312–322.
- (51) Abe, M.; Kitagawa, T.; Kyogoku, Y. *J. Chem. Phys.* **1978**, *69*, 4526–4534.
- (52) Li, X. Y.; Czernuszewicz, R. S.; Kincaid, J. R.; Su, Y. O.; Spiro, T. G. *J. Phys. Chem.* **1990**, *94*, 31–47.

Table 1. Percentage Overlap of Calculated Modes with Porphyrin Core Normal Modes and Ligand Vibrations^a

freq	ampl (pm)	asgmt	ν_{42a}	ν_{42b}	ν_{49a}	ν_{49b}	ν_{50a}	ν_{50b}	ν_{53a}	ν_{53b}	γ_6	γ_9	ν_{FeC}	δ_{FeCO}	ν_{FeIm}	$\delta_{FeImCim}$
33	3.56	phenyl					1	1		1	31	11	21	4	2	
53	1.07	phenyl	4	1	7	7	11	12	8	7		1				
55	1.03	phenyl	4	9	6	7	11	10	8	9		3		7	1	3
69	0.76	$\gamma_{9,6}$	1				4	6	5	6	15	40	6	4	3	4
75	0.66	$\gamma_{9,6}$	1				5	2	5	2	14	21	6	14		3
76	0.63	$\gamma_{9,6}$	1				4	3	4	4	13	17	6	5		3
124	0.77	$\gamma_{9,6}$	2	3				7		9	24	31	9	17	14	5
172	0.80	$\delta_{Fe-imid}$	3	8	4	4	5	6	7	11	16	7	8	6	15	56
226	1.33	ν_{FeHis}	1	16	6	7	3	1	7	10	41	6	18	20	64	9
244	1.32	$\nu_{42,49,50}$	20	8	15	16	16	12	6	1	4		2	1	4	4
255	1.03	$\nu_{42,49,50}$	4	27	18	12	13	28	1	3	18	2	5	7	15	15
301	0.87		6	5	16	10	7	15	8	21	22	17	11	45	18	7
325	2.11	$\nu_{49,53}$	13	13	20	43	24	4	52	8			1	4		7
338	1.77	$\nu_{49,53}$	12	16	40	17	3	10	5	51	9	8	4	14		7
384	0.49		7	11	9	4	41	7	14	4						8
410	0.71	$\nu_{50,53}$	8	7	8	16	62	7	31	3				1		5
420	0.83	$\nu_{50,53}$	7	7	8	9	6	59	1	23	3	4	2	7		11
470	0.62	$\nu_{49,53}$	7	17	60	56	5	8	24	25			3	10	2	7
471	0.69	$\nu_{49,53}$	10	8	54	58	7	9	25	22			2	5	1	
506	1.29	ν_{FeC}	2	3	6	3	1	5		3	31	20	49	21	40	7
569	0.63	δ_{FeCO}	6	6	10	6	3	11	3	8	13	4	15	75	19	14
591	1.01	δ_{FeCO}	4	4	6	4	2	7	2	6	27	23	34	64	40	6

^a The numbers indicate the scalar product of true [Fe(TPP)(CO)(1-MeIm)] normal modes with the model eigenvectors corresponding to the γ , ν , or ligand vibrations. The Fe amplitude at 20 K is also given for each mode.

by first constructing normalized mass-weighted vectors representing elements of the set. Subsequently, inner products of the calculated eigenvectors with those vectors determine the overlap of the [Fe(TPP)(CO)(1-MeIm)] normal modes. Table 1 shows the extent of overlap of [Fe(TPP)(CO)(1-MeIm)] iron modes with various modes of the reference set. As a result of strong coupling of phenyls, imidazole, and CO units with the porphyrin core, [Fe(TPP)(CO)(1-MeIm)] normal modes are found to have large overlap with multiple reference modes. The significant overlap of each [Fe(TPP)(CO)(1-MeIm)] mode with so many modes of the porphyrin core demonstrates the limitation of labeling the actual modes in terms of the conventional porphyrin core modes.

Further information on the character of the [Fe(TPP)(CO)(1-MeIm)] modes is obtained from their PED, shown in Table 2. For a given mode, the PED describes the contributions of various internal coordinates of the system to its potential energy, and reveals the relative contributions of the phenyl, imidazole, CO ligand, and porphyrin core force constants.

The best-fit calculation is used to characterize the observed iron modes of [Fe(TPP)(CO)(1-MeIm)]. As shown in Figure 3, good agreement between the calculated and experimental iron VDOS is achieved over a wide range of frequency. The disagreement between calculation and experiment in the low-frequency region (below ~ 50 cm^{-1}) is due to our single molecule model of [Fe(TPP)(CO)(1-MeIm)], which does not incorporate intermolecular interactions and crystal field effects that are expected to play important roles at low frequencies. Acoustic modes involving large displacements of iron are likely to contribute to the broad asymmetric feature around 30 cm^{-1} .

The following discussion of the [Fe(TPP)(CO)(1-MeIm)] iron vibrational modes is grouped as follows: (a) in-plane modes of the porphyrin core (ν_{42} , ν_{49} , ν_{50} , ν_{53}); (b) Fe–CO stretch and bend modes; (c) iron-imidazole vibrations; (d) phenyl modes; (e) and porphyrin core out-of-plane modes (doming and pyrrole tilting).

A. In-Plane Porphyrin Modes. In D_{4h} symmetric porphyrins the in-plane modes with finite iron displacements are of E_u

Table 2. Calculated Modes and Potential Energy Distribution^a

freq (cm^{-1})	mode assignment	PED (%)
33	phenyl, op	$\delta_{FeCO}(33)$
53	phenyl, ip	$\delta_{C_{\alpha}C_{\beta}C_{\gamma}C_{\delta}}(20) + \delta_{C_{\alpha}C_{\beta}C_{\gamma}C_{\delta}}(20) + \tau_{C_{\alpha}C_{\beta}C_{\gamma}C_{\delta}}(12) + \tau_{C_{\alpha}C_{\beta}C_{\gamma}C_{\delta}}(12)$
55	phenyl, ip	$\delta_{C_{\alpha}C_{\beta}C_{\gamma}C_{\delta}}(21) + \delta_{C_{\alpha}C_{\beta}C_{\gamma}C_{\delta}}(20) + \tau_{C_{\alpha}C_{\beta}C_{\gamma}C_{\delta}}(12) + \tau_{C_{\alpha}C_{\beta}C_{\gamma}C_{\delta}}(12)$
69	$\gamma_{9,6}$, op	$\delta_{FeCO}(42) + \delta_{N_{Fe}FeC}(5) + \delta_{N_{Fe}FeC}(4)$
75	$\gamma_{9,6}$, op	$\delta_{FeCO}(23) + \delta_{N_{Fe}FeC}(6)$
76	$\gamma_{9,6}$, op	$\delta_{FeCO}(15) + \delta_{N_{Fe}FeC}(5)$
124	$\gamma_{9,6}$, op	$\nu_{FeNim}(6) + \delta_{N_{Fe}FeC}(7) + \delta_{N_{Fe}FeC}(28)$
172	$\delta_{Fe-imid}$, ip	$\delta_{FeNimCim}(36) + \delta_{N_{Fe}FeC}(8)$
226	$\nu_{Fe-imid}$, op	$\nu_{FeC}(8) + \nu_{FeNim}(35) + \delta_{FeCO}(7) + \delta_{C_{im}N_{im}C_{im}}(7)$
244	$\nu_{42,50}$, ip	$\tau_{C_{\alpha}C_{\beta}C_{\gamma}C_{\delta}}(4) + \tau_{C_{\alpha}C_{\beta}C_{\gamma}C_{\delta}}(4)$
255	$\nu_{42,50}$, ip	$\tau_{C_{\alpha}C_{\beta}C_{\gamma}C_{\delta}}(7) + \tau_{C_{\alpha}C_{\beta}C_{\gamma}C_{\delta}}(7)$
301	ip, op	$\nu_{FeN_{Fe}}(9) + \delta_{FeCO}(20) + \delta_{C_{\alpha}C_{\beta}C_{\gamma}C_{\delta}}(4) + \delta_{C_{\alpha}C_{\beta}C_{\gamma}C_{\delta}}(6)$
325	$\nu_{49,53}$, ip	$\nu_{FeN_{Fe}}(13) + \nu_{FeN_{Fe}}(16)$
338	$\nu_{49,50,53}$, ip	$\nu_{FeN_{Fe}}(4) + \nu_{FeN_{Fe}}(14) + \delta_{C_{im}N_{im}C_{im}}(5)$
384	ip	$\nu_{FeN_{Fe}}(5) + \nu_{FeN_{Fe}}(5) + \delta_{C_{im}N_{im}C_{im}}(6) + \gamma_{H_{Fe}C_{Fe}C_{Fe}}(52)$
410	$\nu_{50,53}$, ip	$\nu_{FeN_{Fe}}(10) + \nu_{FeN_{Fe}}(10)$
420	$\nu_{50,53}$, ip	$\nu_{FeN_{Fe}}(10) + \nu_{FeN_{Fe}}(12)$
470	$\nu_{49,53}$, ip	$\delta_{C_{\alpha}C_{\beta}C_{\gamma}C_{\delta}}(4) + \delta_{C_{\beta}C_{\gamma}C_{\delta}}(4) + \delta_{C_{\alpha}C_{\beta}C_{\gamma}C_{\delta}}(4) + \delta_{C_{\beta}C_{\gamma}C_{\delta}}(4) + \delta_{C_{\alpha}C_{\beta}C_{\gamma}C_{\delta}}(4)$
471	$\nu_{49,53}$, ip	$\delta_{C_{\alpha}C_{\beta}C_{\gamma}C_{\delta}}(4) + \delta_{C_{\alpha}C_{\beta}C_{\gamma}C_{\delta}}(4) + \delta_{C_{\beta}C_{\gamma}C_{\delta}}(4) + \delta_{C_{\beta}C_{\gamma}C_{\delta}}(4)$
506	ν_{FeC} , op	$\nu_{FeC}(44) + \delta_{N_{im}C_{im}C_{im}}(10) + \delta_{N_{im}C_{im}C_{im}}(7) + \delta_{C_{im}N_{im}C_{im}}(10)$
569	δ_{FeCO} , ip	$\nu_{FeC}(4) + \nu_{FeNim}(13) + \delta_{FeCO}(23) + \delta_{N_{im}C_{im}C_{im}}(12) + \delta_{C_{im}N_{im}C_{im}}(13)$
591	δ_{FeCO} , ip	$\nu_{FeC}(7) + \nu_{FeNim}(17) + \delta_{FeCO}(17) + \delta_{N_{im}C_{im}C_{im}}(8) + \delta_{C_{im}N_{im}C_{im}}(10)$

^a The contribution to the potential energy of a particular normal mode from stretch(ν), angle bend(δ), torsion(τ), and out-of-plane bend(γ) force constants is shown. The number in the bracket indicates the percentage contribution of a given force constant to the PED of the mode. In-plane and out-of-plane motions are indicated by ip and op, respectively. Only those force constants which contribute 4% or more to the PED are listed.

symmetry type, which are doubly degenerate and Raman inactive. Recently, the porphyrin in-plane modes with ν_{42} , ν_{50} , and ν_{53} character in heme model compounds [Fe(TPP)(NO)] and [Fe(TPP)(2-MeHIm)] have been identified using NRVs.^{26,27}

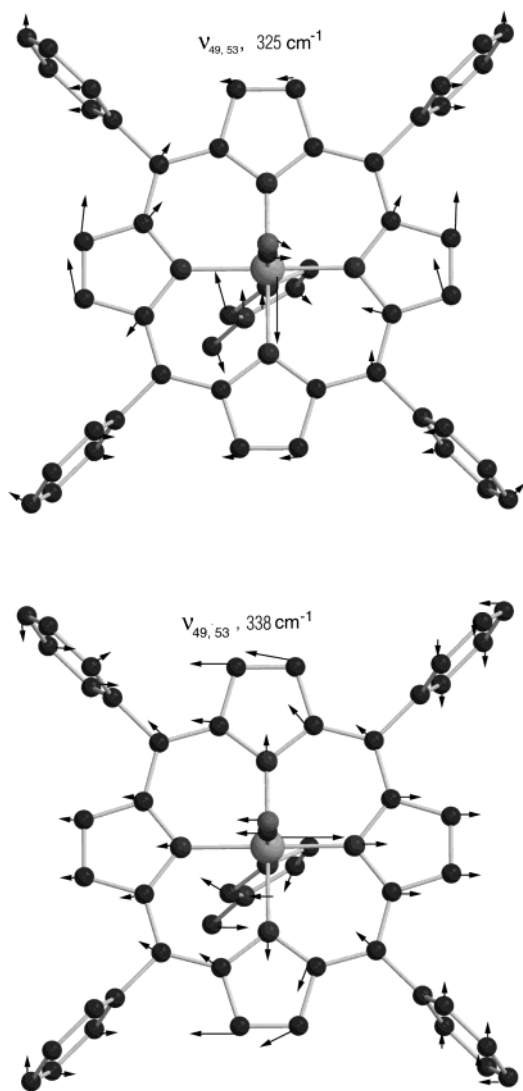


Figure 5. Eigenvectors of in-plane modes at 325 and 338 cm^{-1} . The lengths of the arrows indicate relative magnitudes of atom displacements within the heme plane.

The frequencies of these modes in the two heme compounds were found to be very similar. The in-plane character of the porphyrin modes in [Fe(TPP)(NO)] and [Fe(TPP)(2-MeHIm)] was confirmed experimentally by NRVS measurements on oriented crystals. Although the [Fe(TPP)(CO)(1-MeIm)] data were only obtained from polycrystalline materials, the calculated in-plane assignments are in good agreement with results from the other two model compounds.

The most prominent feature of the iron VDOS (Figure 3) is a doublet with peaks at 325 and 338 cm^{-1} ; normal mode refinement establishes these as having largely ν_{53} character. This mode is defined as an in-plane displacement of iron which is opposed by the translational motion of the two pyrrole rings situated directly opposite to each other. The characters of the two modes, ν_{53a} and ν_{53b} , are shown in Figure 5. The 2-fold degeneracy of this mode is apparently lifted as a result of the imidazole and CO ligand coupling with the porphyrin core. The ν_{53b} mode couples to the Fe–C–O bending vibration, and it shifts to a higher frequency (341 cm^{-1}) compared to the ν_{53a} mode. The iron amplitude in ν_{53b} mode is smaller than that in

ν_{53a} mode as the whole FeCO unit in this case opposes the displacement of pyrrole rings.

The frequencies and iron amplitudes of the ν_{53} modes in [Fe(TPP)(CO)(1-MeIm)] are similar to those previously observed in [Fe(TPP)(NO)].²⁶ The splitting of the ν_{53} mode in [Fe(TPP)(NO)] was attributed to a coupling of Fe–N–O bending motion with the vibration of the porphyrin core. In absence of a diatomic ligand the ν_{53} mode in 5-coordinate [Fe(TPP)(2-MeHIm)], which has an imidazole ring as its fifth ligand, does not show a discernible splitting. The PEDs of the ν_{53} modes have the largest contributions from the Fe–N_p force constants. Thus, a comparison of the ν_{53} mode frequencies of the three heme compounds [Fe(TPP)(NO)], [Fe(TPP)(2-MeHIm)], and [Fe(TPP)(CO)(1-MeIm)] gives some insight into relative strength of the Fe–N_p bonds. As mentioned before, the ν_{53a} mode in [Fe(TPP)(NO)] or [Fe(TPP)(CO)(1-MeIm)] does not couple with the Fe–C–O or Fe–N–O ligand vibration. The frequency of the ν_{53a} mode in these two compounds is very similar, 313 cm^{-1} for [Fe(TPP)(NO)] and 319 cm^{-1} for [Fe(TPP)(CO)(1-MeIm)]. However, the analogous modes with ν_{53} character in [Fe(TPP)(2-MeHIm)], which are observed to be nearly degenerate, are calculated to occur at somewhat lower frequencies (288 and 293 cm^{-1}). The stiffened force constants in [Fe(TPP)(CO)(1-MeIm)], consistent with the differences in spin state and shorter Fe–N_p distances compared to [Fe(TPP)(2-MeHIm)], lead to higher ν_{53} frequencies in [Fe(TPP)(CO)(1-MeIm)].

In addition to the ν_{53} modes, the normal mode calculations identify three other E_u modes having somewhat smaller iron amplitudes. The observed features in the iron VDOS at ~ 250 , ~ 410 , and ~ 470 cm^{-1} are assigned to a combination of doubly degenerate ν_{42} , ν_{50} , and ν_{49} modes. The character of the doublet at 410 cm^{-1} , having large overlaps with ν_{50} and ν_{53} modes, are shown in Figure 6. Figure 7 shows the eigenvectors of the pair of modes at 244 and 255 cm^{-1} modes. The character of the doublet at 470 cm^{-1} overlaps with pyrrole translation (ν_{53}) and pyrrole rotation (ν_{49}) coordinates of the porphyrin core (Figure 8).

B. Fe–CO Ligand. The normal-mode analysis identifies three modes from our experimental VDOS spectrum that arise from vibrations of the Fe–CO system, Fe–C stretch at 506 cm^{-1} and the Fe–C–O bend doublet at 561 and 587 cm^{-1} . Similar modes in carbonmonoxy myoglobin and hemoglobin have been previously observed from Raman measurements, generally at slightly higher energies.^{20,22} Recent NRVS measurements on MbCO also indicate the presence of Fe–CO ligand modes in the 500–600 cm^{-1} region (see Figure 4 for a comparison).^{6,53} Note that each of the Fe–CO ligand modes have very large overlaps with the γ_6 and γ_9 out-of-plane porphyrin core modes. This suggests that the γ_6 and γ_9 modes may play an important role in porphyrin-ligand binding.

Density functional theory (DFT) calculations have been reported for a very similar structure, [Fe(porphine)(Im)CO].⁵⁰ The three Fe–CO modes seen in the NRVS data (at 506, 561, and 587 cm^{-1}) are calculated to be at 501, 572, and 578 cm^{-1} , in reasonably good agreement with the NRVS and with Raman data.

C. Iron Imidazole Vibrations. The iron-imidazole stretch mode is Raman active in deoxy states of Mb, Hb, and certain

(53) Achterhold, K.; Keppler, C.; Ostermann, A.; van Bürck, U.; Sturhahn, W.; Alp, E. E.; Parak, F. *Phys. Rev. E* **2002**, *65*, 051 916.

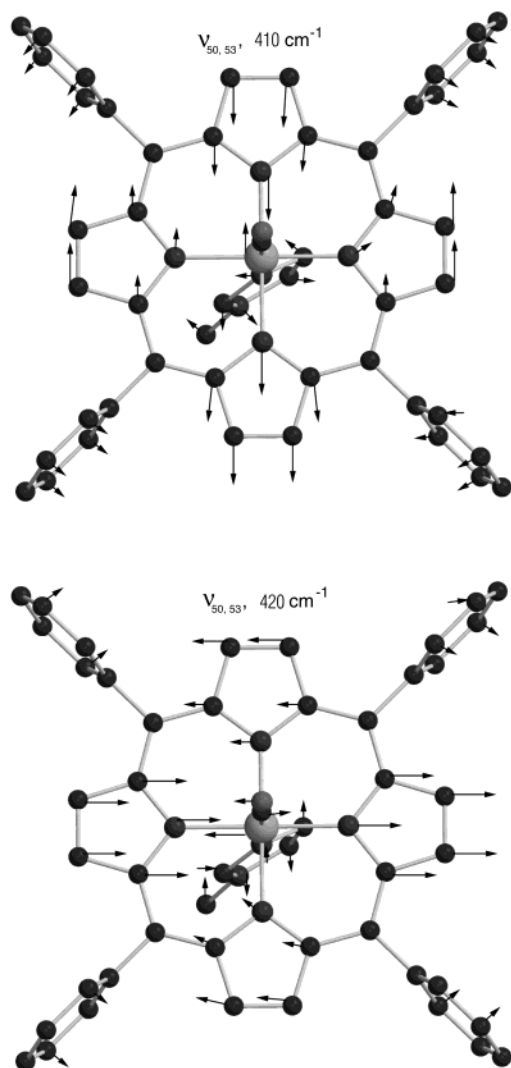


Figure 6. The eigenvector of in-plane modes at 410 and 420 cm^{-1} . These modes show significant overlap with ν_{50} and ν_{53} porphyrin core vibrations. The lengths of the arrows indicate relative magnitudes of atom displacements within the heme plane.

model compounds, but cannot be seen with Raman when CO (and other small ligands) binds to the Fe, forcing the Fe atom to be coplanar with the porphyrin. It has always been something of a mystery to discern how the Fe-imidazole frequency changes upon ligand binding, as it has never been observed with optical probes. It is important to accurately characterize the iron-imidazole modes, as the iron-imidazole bond in Mb and Hb is the only covalent connection of the heme with the protein.

Numerous flash-photolysis experiments on Mb and Hb have shown a higher frequency of the Fe–His mode in the deoxy R state than in the deoxy T state.⁵⁴ The Fe–His vibrational frequency is also known to decrease with time after the flash-photolysis of carbonmonoxy Mb and Hb. The fully relaxed deoxy states of Mb or Hb show the frequency of the Fe–His mode in the range of 210–220 cm^{-1} . Using NRVS we found this mode in the deoxy heme model [Fe(TPP)(2-MeHIm)] at 215 cm^{-1} . The NRVS spectrum of the carbonmonoxy model compound, [Fe(TPP)(CO)(1-MeIm)], shows three distinct peaks in the 200–260 cm^{-1} region. We have already assigned the

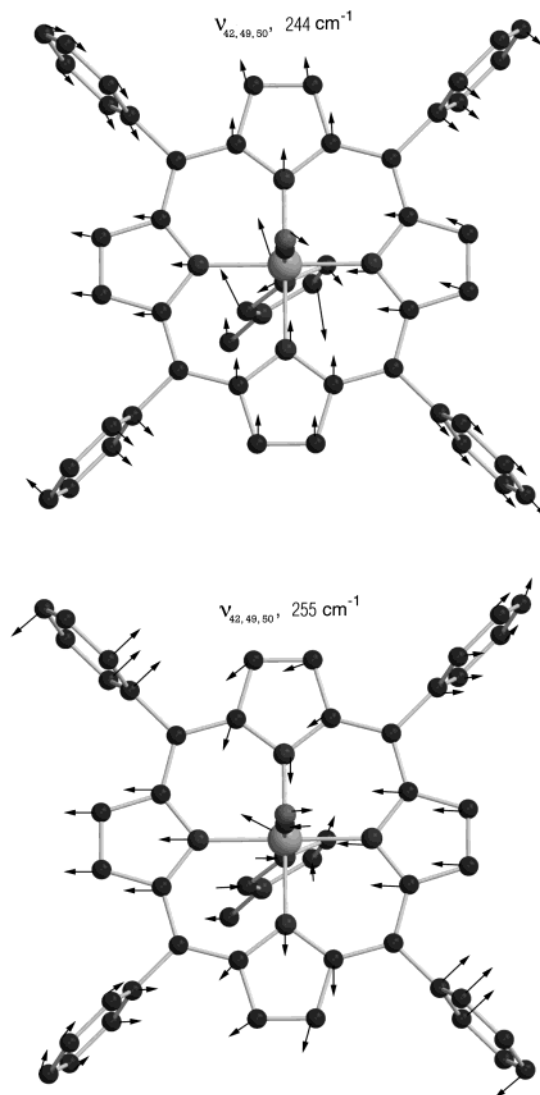


Figure 7. Eigenvector of modes at 244 and 255 cm^{-1} . The lengths of the arrows indicate relative magnitudes of atom displacements within the heme plane.

modes at 244 and 255 cm^{-1} to in-plane vibrations of the porphyrin core. The remaining mode at 226 cm^{-1} is the iron-imidazole stretch mode (see Table 1). The character of the iron-imidazole stretch mode is shown in Figure 9. Normal-mode analysis shows a 35% iron-imidazole stretch contribution to the PED of the 226 cm^{-1} mode. Smaller contributions to the PED come from Fe–C stretch, and Fe–C–O bend force constants. The relatively small differences in the iron-imidazole stretch in [Fe(TPP)(CO)(1-MeIm)] and the five-coordinate complex is perhaps unexpected, in light of the decrease of the Fe–N_{Im} bond distances in [Fe(TPP)(CO)(1-MeIm)] (2.071 Å)¹⁵ from that of [Fe(TPP)(2-MeHIm)] (2.127 Å).¹⁶ Additional measurements to explore this mode are planned.

The normal mode calculation also yields modes at 69, 75, and 76 cm^{-1} that have their largest PED contributions from bending of the CO ligand and the imidazole, as well as some overlap with the γ_9 and γ_6 core modes. These modes are apparently identical to the 70, 73, and 74 cm^{-1} modes predicted by DFT in [Fe(porphine)(Im)CO].⁵⁰ These modes cannot be individually identified in the NRVS data (although a clear band of extra states is visible), nor have they been reported by other

(54) Rousseau, D. L.; Friedman, J. M. *Biological Application of Raman Spectroscopy*; Wiley-Interscience: New York, 1988; Vol. 3.

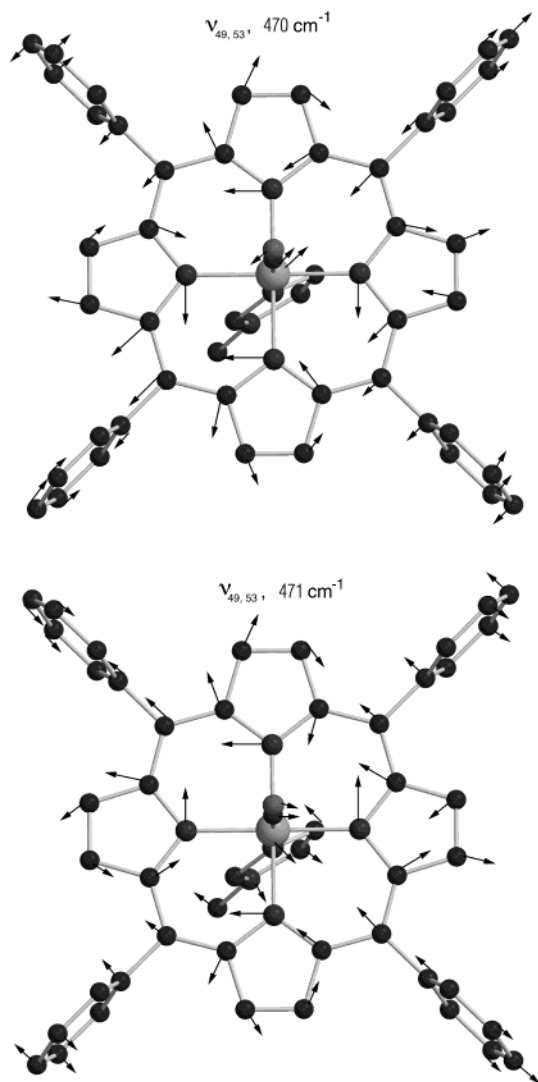


Figure 8. Eigenvector of the doublet at 470 and 471 cm^{-1} . The lengths of the arrows indicate relative magnitudes of atom displacements within the heme plane.

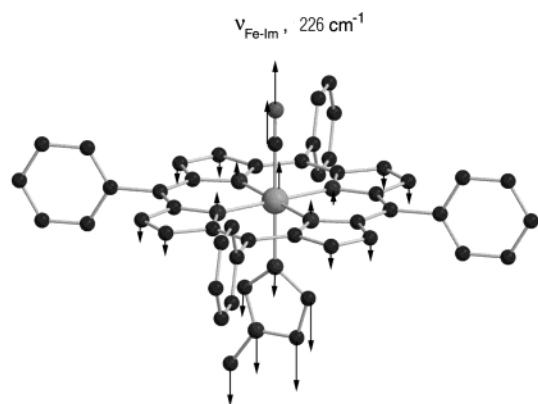


Figure 9. Eigenvector of out-of-plane iron-imidazole stretch mode at 226 cm^{-1} . The lengths of the arrows indicate relative magnitudes of atom displacements perpendicular to the heme plane.

spectroscopies. Their independent predictions by DFT and by this normal mode fit to the data certainly strengthens the case for their existence.

The experimental mode at 172 cm^{-1} is also identified as a bending motion of the imidazole ring. The $\text{Fe}-\text{N}_{\text{Im}}-\text{C}_{\text{Im}}$ force

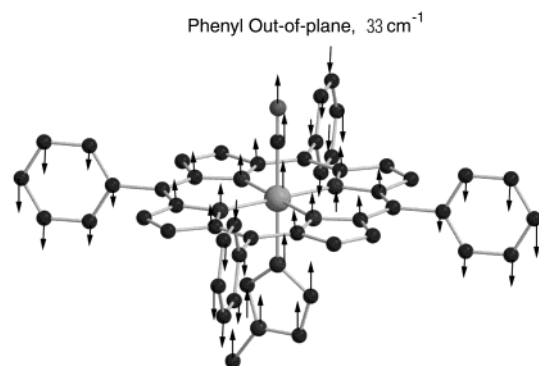


Figure 10. Phenyl out-of-plane mode at 33 cm^{-1} . The lengths of the arrows indicate relative magnitudes of atom displacements perpendicular to the heme plane.

constants contribute 36% to the PED of this mode. This mode is quite distinct in the NRVS data, but it does not appear to have been previously reported. The absence of this bending mode from RR and IR spectra again highlights the severe constraints imposed by the optical selection rules associated with these techniques. In the absence of any such selection rules in NRVS, this mode is very prominently observed in our measurements. We note that other metalloporphyrin-imidazole complexes have been reported with imidazole bends greater than 10° away from the heme normal.^{55–57} These large bends may be activated by the type of bending modes seen here for the first time.

D. Phenyl Modes. The coupling of the phenyl vibrations with the porphyrin core results in three normal modes involving significant displacements of iron. Two of these phenyl modes near 55 cm^{-1} involve in-plane displacement of iron and are nearly degenerate. The iron displacements in these modes are essentially perpendicular to each other along a line bisecting the $\text{N}_p-\text{Fe}-\text{N}_p$ angle, and are opposed by a lateral motion of two phenyls on the opposite side of the porphyrin center. The third mode at 33 cm^{-1} involves a large out-of-plane displacement of iron, which is opposed by oscillations of phenyl rings perpendicular to the heme plane (Figure 10). This mode has an Fe out-of-plane displacement of 3.56 pm, largest of all the normal modes (see Table 1).

The contribution of phenyls to the dynamics of NiTPP has previously been considered in a comparison of DFT predictions with RR and IR spectra³. Because these optical spectroscopies are not normally effective below about 150 cm^{-1} , no data or DFT results are reported. The NRVS analysis, on the other hand, has revealed the critical role of the phenyls in causing the largest iron atom displacement of any mode, at 33 cm^{-1} .

E. Porphyrin Core Out-of-Plane Modes. Biologically significant out-of-plane modes of heme model compounds [Fe(TPP)(NO)] and [Fe(TPP)(2-MeHIm)] have previously been studied using NRVS. The low frequency heme modes involving out-of-plane displacement of iron are Raman inactive and are difficult to identify using IR techniques. Porphyrin core out-of-plane modes in [Fe(TPP)(NO)] and [Fe(TPP)(2-MeHIm)] show essentially similar characteristics, with modes near 70 and 130 cm^{-1} corresponding to a combination of doming and pyrrole tilting.

(55) Freeman, H. C. *Adv. Protein Chem.* **1967**, 22, 257–425.

(56) Scheidt, W. R. *J. Am. Chem. Soc.* **1974**, 96, 90–94.

(57) Kirner, J. F.; Reed, C. A.; Scheidt, W. R. *J. Am. Chem. Soc.* **1977**, 99, 2557–2563.

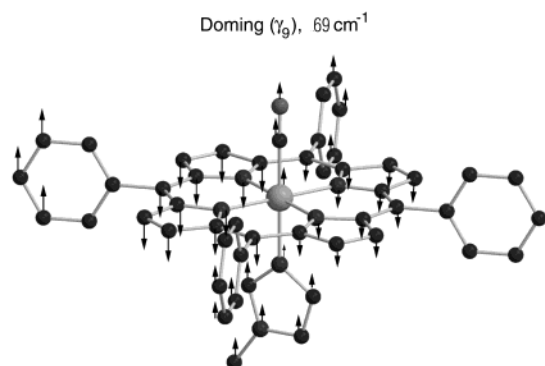


Figure 11. Eigenvector of out-of-plane doming (γ_9) mode at 69 cm^{-1} . The lengths of the arrows indicate relative magnitudes of atom displacements in the heme normal direction. As indicated in Table 2, there is also significant bending of the Fe–C–O unit associated with this mode.

The NRVS spectrum of $[\text{Fe}(\text{TPP})(\text{CO})(1\text{-MeIm})]$ shows a band near 70 cm^{-1} and another peak at 124 cm^{-1} that both have significant overlap with doming and pyrrole tilting coordinates, i.e., the γ_9 and γ_6 porphyrin core modes. The band near 70 cm^{-1} is fitted by peaks at 69 , 75 , and 76 cm^{-1} , each with large contributions from the γ_9 and γ_6 modes. The doming and the pyrrole tilting coordinates contribute nearly equally to the 124 cm^{-1} mode, with the overlap of γ_9 and γ_6 modes at 31 and 24% . In addition, the doming and pyrrole tilting coordinates strongly couple with the fifth (imidazole) and sixth (CO) ligands. The eigenvector of the out-of-plane mode at 69 cm^{-1} is shown in Figure 11.

In adjusting the force constants to get good fits at both the 124 cm^{-1} mode and the band of modes near the calculated lines at 69 , 75 , and 76 cm^{-1} , it was necessary to adjust the interaction between the FeCO bend and $\text{N}_\text{P}\text{FeC}$ tilting force constants. The adjustment requires a negative interaction force constant between the tilting and bending modes. The magnitude of this interaction force constant ($-0.34\text{ mdy}\cdot\text{\AA}/\text{rad}^2$) is similar to values previously reported (i.e., -0.40 ⁵⁸ and -0.26 ²⁵ ($\text{mdyn}\cdot\text{\AA}/\text{rad}^2$)). Importantly, the necessity of this negative force constant to fit our NRVS data provides confirmation of the suggestion of Ghosh and Bocian⁵⁸ that the combination of tilting and bending provides a soft mode for Fe–C–O distortion.

V. Conclusions

In conjunction with previous work on a deoxy heme model compound,²⁷ this study in particular has illuminated the impact of ligand binding on the dynamics of the active Fe site in a carbonmonoxy-heme model compound. The association of the CO ligand to the heme activates a number of iron modes that are either weak or absent in the iron VDOS of the deoxy heme compound. The most pronounced effect is observed on the porphyrin in-plane modes with primarily ν_{53} character. The degeneracy of the ν_{53} mode, which is doubly degenerate in the porphyrin core, is lifted by the coupling of the ν_{53b} mode with the CO ligand. The higher frequency of the ν_{53} modes in carbonmonoxy heme as compared to that in deoxy heme is a

direct consequence of the heme structural changes in which the iron atom moves from its domed position in deoxy heme toward the heme plane upon CO ligand binding, decreasing the Fe– N_P bond lengths from 2.073 \AA in $[\text{Fe}(\text{TPP})(2\text{-MeHIm})]$ ¹⁶ to 2.003 \AA in $[\text{Fe}(\text{TPP})(\text{CO})(1\text{-MeIm})]$.¹⁵

Our unique identification of the Fe–His mode in carbonmonoxy heme at 226 cm^{-1} again highlights the effectiveness of NRVS as a technique to study iron vibrations. This mode is Raman inactive in the carbonmonoxy state of Mb, Hb and heme model compounds and, despite considerable effort, has not been observed before. In addition, we also identify a previously unsuspected Fe-imidazole bending mode at 172 cm^{-1} . The Fe–C stretch and Fe–C–O bending modes in our NRVS data appear close to their Raman values at 506 and $561/587\text{ cm}^{-1}$. We also identify modes near $69\text{--}76\text{ cm}^{-1}$ and at 124 cm^{-1} due to out-of-plane motion of iron; the lower frequency modes also have significant imidazole bending, consistent with DFT predictions. The largest doming motion of the Fe is predicted to occur for a phenyl mode at 33 cm^{-1} , suggesting that the outer substituents of the porphyrin might have a bigger role in heme dynamics than previously known.

Overall, these results provide a sound starting point for describing Fe dynamics in heme proteins, especially carbonmonoxy-myoglobin and carbonmonoxy-hemoglobin. This investigation demonstrates that NRVS data can be used to determine the force field for the heme molecule by a best fit refinement, and that the resultant normal modes provide a highly plausible description of the characteristics of the individual normal modes. This procedure is a major advance, at least with regards to modes involving significant iron atom motion, due to the greater number of experimental constraints provided by NRVS as compared to standard optical spectroscopies. The frequencies of all modes with iron motions are determined, up to about 700 cm^{-1} , and the amplitude of each experimental mode is also determined by the data. Most important, the method is 100% selective for the iron atom alone; no other atoms can be detected. When combined with existing results of many systematic RR and IR studies of various heme compounds, and comparing with DFT calculations, these data and the associated normal mode calculation produce a substantially more complete picture of iron dynamics in heme molecules.

Acknowledgment. We thank K. Adams and C. Zhang for their assistance with taking the NRVS data, and J. Zhao for expert beam line support at the Advanced Photon Source. This work was supported by the National Science Foundation through Award No. PHY-9988763 (for authors B.K.R., S.D., and E.W.P.) and No. PHY-99-83100 (J.T.S.), and by the National Institutes of Health through Grant Nos. GM-38401 (M.K.E., A.R., and W.R.S.) and GM-52002 (J.T.S.). B.K.R. and E.W.P. acknowledge support from the Mobile Manufacturer's Forum, and B.K.R. also acknowledges support from the Purdue Research Foundation. Use of the Advanced Photon Source was supported by the U. S. Department of Energy, Basic Energy Sciences, Office of Science, under Contract No. W-31-109-Eng-38.

(58) Ghosh, A.; Bocian, D. F. *J. Phys. Chem.* **1996**, *100*, 6363–6367.

(59) Scheidt, W. R.; Duval, H. F.; Neal, T. J.; Ellison, M. K. *J. Am. Chem. Soc.* **2000**, *122*, 4651–4659.